Journal of Applied Fluid Mechanics, Vol. 9, No. 4, pp. 1667-1678, 2016.
Available online at www.jafmonline.net, ISSN 1735-3572, EISSN 1735-3645.
DOI: 10.18869/acadpub.jafm.68.235.24718

Free Convection Flow and Heat Transfer of Tangent Hyperbolic past a Vertical Porous Plate with Partial Slip

V. Ramachandra Prasad[1], S. Abdul Gaffar[2†] and O. Anwar Beg[3]

[1]*Department of Mathematics, Madanapalle Institute of Technology and Science, Madanapalle-51732, India*
[2]*Department of Mathematics, Salalah College of Technology, Salalah, Oman*
[3]*Gort Engovation Research (Aerospace), 15 Southmere Avenue, Great Horton, Bradford, BD7 3Nu, West Yorkshire, UK*

†*Corresponding Author Email: abdulsgaffar0905@gmail.com*

(Received February 19, 2015; accepted August 4, 2015)

ABSTRACT

This article presents the nonlinear free convection boundary layer flow and heat transfer of an incompressible Tangent Hyperbolic non-Newtonian fluid from a vertical porous plate with velocity slip and thermal jump effects. The transformed conservation equations are solved numerically subject to physically appropriate boundary conditions using a second-order accurate implicit finite-difference Keller Box technique. The numerical code is validated with previous studies. The influence of a number of emerging non-dimensional parameters, namely the Weissenberg number (We), the power law index (n), Velocity slip (Sf), Thermal jump (ST), Prandtl number (Pr) and dimensionless tangential coordinate (ξ) on velocity and temperature evolution in the boundary layer regime are examined in detail. Furthermore, the effects of these parameters on *surface heat transfer rate* and *local skin friction* are also investigated. Validation with earlier *Newtonian* studies is presented and excellent correlation achieved. It is found that velocity, skin friction and heat transfer rate (Nusselt number) is increased with increasing Weissenberg number (We), whereas the temperature is decreased. Increasing power law index (n) enhances velocity and heat transfer rate but decreases temperature and skin friction. An increase in Thermal jump (S_T) is observed to decrease velocity, temperature, local skin friction and Nusselt number. Increasing Velocity slip (S_f) is observed to increase velocity and heat transfer rate but decreases temperature and local skin friction. An increasing Prandtl number, (Pr), is found to decrease both velocity and temperature. The study is relevant to chemical materials processing applications.

Keywords: Non-newtonian tangent hyperbolic fluid; Boundary layer flow; Weissenberg number; Power law index; Velocity slip; Thermal jump; Skin friction; Nusselt number.

NOMENCLATURE

C_f	skin Friction Coefficient
F	dimensionless stream function
Gr_x	Grashof number
g	acceleration due to gravity
k	thermal conductivity of the fluid
K_0	thermal Jump factor
n	power law index
N_0	velocity slip factor
Nu	local Nusselt number
Pr	Prandtl number
S_f	dimensionless Velocity Slip parameter
S_T	dimensionless Thermal Jump parameter
T	fluid temperature
u, v	dimensionless velocity components along the x - and y – directions, respectively
V	velocity vector
We	Weissenberg number
x	stream wise coordinate
y	transverse coordinate
α	thermal diffusivity
β	coefficient of thermal expansion
ν	kinematic viscosity
ρ	fluid density
μ	dynamic viscosity
η	dimensionless radial coordinate
θ	dimensionless Temperature
ξ	dimensionless tangential coordinate
ψ	dimensionless Stream function
Γ	time dependent material constant
Π	second invariant strain tensor

Subscripts

w	surface conditions on plate (wall)
∞	free Stream conditions

1. INTRODUCTION

Interest in boundary layer flows of non-Newtonian fluids has been increased due to their applications in science, engineering including thermal oil recovery, food and slurry transportation, polymer and food processing. A variety of non-Newtonian fluid models have been proposed in the literature keeping in view of their several rheological features. In these fluids, the constitutive relationship between stress and rate of strain is non-linear in comparison to the Navier-Stokes equations which are generally good for Newtonian fluids. Non-Newtonian transport phenomena arise in many branches of process mechanical, chemical and materials engineering. Most non-Newtonian models involve some form of modification to the momentum conservation equations. These include power-law fluids (2012), viscoelastic fluids including Johnson-Segalman liquids (2013), Walters-B short memory models (2011), Oldroyd-B models (2012) and differential Reiner-Rivlin models (2012). The flow of non-Newtonian fluids in the presence of heat transfer is an important research area due to its relevance to polymer processing and biotechnology (1993; 2001).

The non-adherence of the fluid to a solid boundary is known as velocity slip. It is a phenomenon that has been observed under certain circumstances (1998). The slip flow problem of laminar boundary layer is of considerable practical interest. Microchannels which are at the forefront of today's turbomachinery technologies are widely being considered for cooling of electronic devices, micro heat exchanger systems, etc. If the characteristic size of the flow system is small or the flow pressure is very low, slip flow happens. If the characteristic size of the flow system tends to the molecular mean free path, continuum physics is no longer suitable. In no-slip-flow, as a requirement of continuum physics, the flow velocity is zero at a solid–fluid interface and the fluid temperature instantly closest to the solid walls is equal to that of the solid walls. The fluids exhibiting boundary slip find applications in technology such as in the polishing of artificial heart valves and internal cavities. Slip effects are significant to certain industrial thermal problems and manufacturing fluid dynamics systems. Sparrow *et al.* (1962) presented the first significant investigation of laminar slip-flow heat transfer for tubes with uniform heat flux. Inman (1964) further described the thermal convective slip flow in a parallel plate channel or a circular tube with uniform wall temperature. These studies generally indicated that velocity slip acts to enhance heat transfer whereas temperature jump depresses heat transfer. Many studies have appeared in recent years considering both hydrodynamic and thermal jump effects. Interesting articles of relevance to process mechanical engineering include Larrode *et al.* (2000) who studied thermal/velocity slip effects in conduit thermal convection. Spillane (2007) who examined sheet processing boundary layer flows with slip boundary conditions and Crane and McVeigh (2010) who studied slip hydrodynamics on a micro-scale cylindrical body. Further studies in the context of materials processing include Yu and Ameel (2002), Crane and McVeigh (2010). Studies of slip flows from curved bodies include Bég *et al*. (2011) who examined using network numerical simulation the magneto-convective slip flow from a rotating disk. Wang and Ng (2011) studied using asymptotic analysis of the slip hydrodynamics from a stretching cylinder. Results assuming that the slip solution was a perturbation of the no-slip solution predicted that the slip conditions would not affect shear stress, boundary-layer thickness, or heat transfer (1951; 1952). The solutions to other viscous flows considered similar to boundary layer flows, such as Couette, Poiseuille, and Rayleigh flows, showed a change in heat transfer and shear stress (1967). This led to the suggestion that the mathematical and experimental techniques available at the time lacked the accuracy necessary to capture the result. The suggestion was also made that the boundary-layer equations were not valid for slip flows. Two separate arguments were made. The first was that the second-order slip boundary condition was of the same order as the terms that were discarded from the Navier–Stokes equations to create the boundary-layer equations (1963; 1969). A second problem was the Reynolds number scaling of the boundary-layer equations. Using the definitions of viscosity and the speed of sound, the Knudsen number can be found as a function of the Mach number and Reynolds number (2002):

$$Kn_x \quad \alpha \quad \frac{M}{\mathrm{Re}_x} \tag{1}$$

This scaling indicates that an incompressible boundary layer, with a Reynolds number of 500 or greater and a Mach number of less than 0.3, is unlikely to have a Knudsen number large enough for slip to appear. Several decades after these initial results, the development of microelectromechanical systems led to a renewed interest in slip flows (1998; 1999). The correct scaling of boundary-layer slip was shown to be based on the boundary-layer thickness and was computed as

$$Kn_\delta \quad \alpha \quad \frac{M}{\sqrt{\mathrm{Re}_x}} \tag{2}$$

This scaling does allow an incompressible boundary layer with a Reynolds number of 500 or greater and a Mach number of less than 0.3 to have a large enough Knudsen number for slip to appear. Taking slip flow condition at the boundary, many researchers (2006; 2002; 2002; 2008; 2009) investigated the different flow problems over a stretching sheet. Off late, Chauhan and Olkha (2011) investigated the slip flow of second grade fluid past a stretching sheet in a porous medium by considering the power-law surface temperature/heat flux. Swati Mukhopadhyay and Gorla (2011) studied the effects of partial slip on boundary layer flow past a permeable exponential stretching sheet in presence of thermal radiation. Mukhopadhyay *et al*. (2012) analyzed the Lie group analysis of MHD boundary layer slip flow past a heated stretching

sheet in presence of heat source/sink. Mukhopadhyay and Andersson (2009) studied the Effects of slip and heat transfer analysis of flow over an unsteady stretching surface. Saghafian *et al.* (2015) presented a numerical study on slip flow heat transfer in micro-poiseuille flow using perturbation method. Malvandi *et al.* (2015) studied the boundary layer slip flow and heat transfer of nanofluid induced by a permeable stretching sheet with convective boundary condition.

Convective boundary-layer flows are often controlled by injecting or withdrawing fluid through a porous bounding heat surface. This can lead to enhanced heating or cooling of the system and can help to delay the transition from laminar to turbulent flow. The case of uniform suction and blowing through an isothermal vertical wall was treated first by Sparrow and Cess (1961) they obtained a series solution which is valid near the leading edge. This problem was considered in more detail by Merkin (1972), who obtained asymptotic solutions, valid at large distances from the leading edge, for both the suction and blowing. Using the method of matched asymptotic expansion, the next order corrections to the boundary-layer solutions for this problem were obtained by Clarke (1973), who extended the range of applicability of the analyses by not invoking the usual Boussinesq approximation. The effect of strong suction and blowing from general body shapes which admit a similarity solution has been given by Merkin (1975). A transformation of the equations for general blowing and wall temperature variations has been given by Vedhanayagam *et al.* (1980). The case of a heated isothermal horizontal surface with transpiration has been discussed in some detail first by Clarke and riley (1975; 1976) and then more recently by Lin and Yu (1988). Hossain *et al*. (2001) studied the effect of radiation on free convection flow with variable viscosity from a vertical porous plate.

An interesting non-Newtonian model developed for chemical engineering systems is the Tangent Hyperbolic fluid model. This rheological model has certain advantages over the other non-Newtonian formulations, including simplicity, ease of computation and physical robustness. Furthermore it is deduced from kinetic theory of liquids rather than the empirical relation. Several communications utilizing the Tangent Hyperbolic fluid model have been presented in the scientific literature. There is no single non-Newtonian model that exhibits all the properties of non-Newtonian fluids. Among several non-Newtonian fluids, hyperbolic tangent model is one of the non-Newtonian models presented by Pop and Ingham (2001). Nadeem *et al.* (2009) made a detailed study on the peristaltic transport of a hyperbolic tangent fluid in an asymmetric channel. Nadeem and Akram (2011) investigated the peristaltic flow of a MHD hyperbolic tangent fluid in a vertical asymmetric channel with heat transfer. Akram and Nadeem (2012) analyzed the influence of heat and mass transfer on the peristaltic flow of a hyperbolic tangent fluid in an asymmetric channel. Akbar et al. (2013) analyzed the numerical solutions of MHD boundary layer flow of tangent hyperbolic fluid on a stretching sheet. Very recent studies include V.R. Prasad et al., (2014; 2015; 2015).

The objective of the present study is to investigate the laminar boundary layer flow and heat transfer of a *Tangent Hyperbolic* non-Newtonian fluid past a vertical porous plate. The non-dimensional equations with associated dimensionless boundary conditions constitute a highly nonlinear, coupled two-point boundary value problem. Keller's implicit finite difference "box" scheme is implemented to solve the problems (2014; 2015; 2015; 2012). The effects of the emerging thermophysical parameters, namely *the Weissenberg number (We), power law index (n), Velocity slip (Sf), Thermal jump (ST) and Prandtl number (Pr)* on velocity, temperature, skin friction number and heat transfer rate (local Nusselt number) characteristics are studied. The present problem has to the authors' knowledge not appeared thus far in the scientific literature and is relevant to polymeric manufacturing processes in chemical engineering.

2. NON-NEWTONIAN CONSTITUTIVE TANGENT HYPERBOLIC FLUID MODEL

In the present study a subclass of non-Newtonian fluids known as the *Tangent Hyperbolic fluid* is employed owing to its simplicity. The constitutive equation for *Tangent Hyperbolic* non-Newtonian fluid (2001) takes the form:

$$\bar{\tau} = \left[\mu_\infty + (\mu_0 + \mu_\infty) \tanh\left(\Gamma \bar{\dot{\gamma}} \right)^n \right] \bar{\dot{\gamma}} \tag{1}$$

where $\bar{\tau}$ is extra stress tensor, μ_∞ is the infinite shear rate viscosity, μ_0 is the zero shear rate viscosity, Γ is the time dependent material constant, n is the power law index i.e. flow behavior index and $\bar{\dot{\gamma}}$ is defined as

$$\bar{\dot{\gamma}} = \sqrt{\frac{1}{2}\sum_i \sum_j \bar{\dot{\gamma}}_{ij} \bar{\dot{\gamma}}_{ji}} = \sqrt{\frac{1}{2}\Pi} \tag{2}$$

where $\Pi = \frac{1}{2} trac\left(gradV + (gradV)^T \right)^2$. We consider Eqn. (1), for the case when $\mu_\infty = 0$ because it is not possible to discuss the problem for the infinite shear rate viscosity and since we considering tangent hyperbolic fluid that describing shear thinning effects so $\Gamma \bar{\dot{\gamma}} < 1$. Then Eq. (1) takes the form

$$\bar{\tau} = \mu_0 \left[\left(\Gamma \bar{\dot{\gamma}} \right)^n \right] \bar{\dot{\gamma}} = \mu_0 \left[\left(1 + \Gamma \bar{\dot{\gamma}} - 1 \right)^n \right] \bar{\dot{\gamma}}$$

$$= \mu_0 \left[1 + n \left(\Gamma \bar{\dot{\gamma}} - 1 \right) \right] \bar{\dot{\gamma}} \tag{3}$$

The introduction of the appropriate terms into the flow model is considered next. The resulting boundary value problem is found to be well-posed and permits an excellent mechanism for the assessment of rheological characteristics on the flow behaviour.

3. MATHEMATICAL ANALYSIS

A steady, laminar, two dimensional boundary layer flow and heat transfer of a viscous incompressible tangent hyperbolic fluid over a vertical porous plate is considered, as illustrated in Fig. 1. Both the plate and Tangent Hyperbolic fluid are maintained initially at the same temperature. Instantaneously they are raised to a temperature $T_w > T_\infty$, the ambient temperature of the fluid which remains unchanged.

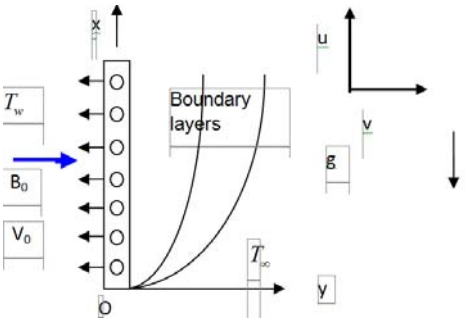

Fig. 1. Physical model and coordinate system.

In line with the approach of Pop and Ingham (2001), Nadeem (2009; 2011; 2012), Akbar (2013), V.R. Prasad *et al*., (2014; 2015) and introducing the boundary layer approximations, the equations for *mass, momentum, and energy*, can be written as follows:

$$\frac{\partial u}{\partial x} + \frac{\partial v}{\partial y} = 0 \tag{4}$$

$$u \frac{\partial u}{\partial x} + v \frac{\partial u}{\partial y} = \nu (1-n) \frac{\partial^2 u}{\partial y^2} + \sqrt{2} \nu n \Gamma \left(\frac{\partial u}{\partial y} \right) \frac{\partial^2 u}{\partial y^2} + g \beta (T - T_\infty) \tag{5}$$

$$u \frac{\partial T}{\partial x} + v \frac{\partial T}{\partial y} = \alpha \frac{\partial^2 T}{\partial y^2} \tag{6}$$

where *u* and *v* are the velocity components in the *x* and *y* directions, respectively, and all the other parameters are mentioned in the nomenclature. The Tangent Hyperbolic fluid model therefore introduces a mixed derivate (second order, first degree) into the momentum boundary layer Eq. (5). The non-Newtonian effects feature in the shear terms only of Eq. (5) and not the convective (acceleration) terms. The thirds term on the right hand side of Eq. (5) represents the thermal buoyancy force and couples the velocity field with the temperature field Eq. (6).

The boundary conditions for the velocity and temperature fields are

$$At \;\; y = 0, \quad u = N_0 \frac{\partial u}{\partial y}, v = 0, \quad T = T_w + K_0 \frac{\partial T}{\partial y}$$
$$As \quad y \to \infty, \quad u \to 0, \quad T \to T_\infty \tag{7}$$

For $N_0 = 0 = K_0$, one can recover the no-slip case. T_w is the convective fluid temperature. The stream function ψ is defined by $u = \frac{\partial \psi}{\partial y}$ and $v = -\frac{\partial \psi}{\partial x}$, and therefore, the continuity equation is automatically satisfied. In order to render the governing equations and the boundary conditions in dimensionless form, the following non-dimensional quantities are introduced

$$\xi = \frac{V_0 x}{\nu} Gr_x^{-1/4}, \eta = \frac{y}{x} Gr_x^{1/4}, \; \psi = 4\nu \sqrt[4]{Gr_x} \left(f(\xi,\eta) + \frac{1}{4}\xi \right)$$
$$\theta(\xi,\eta) = \frac{T - T_\infty}{T_w - T_\infty}, \; \Pr = \frac{\nu}{\alpha}, \; Gr_x = \frac{g\beta(T_w - T_\infty)x^3}{4\nu^2} \tag{8}$$

In view of Eq. (8), the boundary layer Eqs. (5) – (7) reduce to the following coupled, nonlinear, dimensionless partial differential equations for momentum and energy for the regime:

$$(1-n) f''' + (3f + \xi) f'' - 2(f')^2 + n W_e f'' f''' + \theta = \xi \left(f' \frac{\partial f'}{\partial \xi} - f'' \frac{\partial f}{\partial \xi} \right) \tag{9}$$

$$\frac{\theta''}{\Pr} + (3f + \xi)\theta' = \xi \left(f' \frac{\partial \theta}{\partial \xi} - \theta' \frac{\partial f}{\partial \xi} \right) \tag{10}$$

The corresponding transformed boundary conditions are

$$At \;\; \eta = 0, \; f = 0, \; f' = S_f f''(0), \; \theta = 1 + S_T \theta'(0)$$
$$As \;\; \eta \to \infty, \; f' \to 0, \; \theta \to 0 \tag{11}$$

here primes denotes the ordinary differentiation with respect to η, $S_f = \frac{N_0 Gr^{1/4}}{a}$ and $S_T = \frac{K_0 Gr^{1/4}}{a}$ are the dimensionless velocity slip and thermal jump parameters respectively. The wall thermal boundary condition in Eq. (11) corresponds to convective cooling. The skin-friction coefficient (shear stress at the plate surface) and local Nusselt number (heat transfer rate) can be defined with the following expressions.

$$\frac{1}{4} Gr^{-3/4} C_f = (1-n) f''(\xi,0) + \frac{n}{2} W_e (f''(\xi,0))^2 \tag{12}$$

$$Gr^{-1/4} Nu = -\theta'(\xi,0) \tag{13}$$

Table 1 Values of C_f and Nu for different W_e and ξ (Pr = 0.71, n = 0.3, γ = 0.2)

W_e	ξ = 1.0		ξ = 2.0		ξ = 3.0	
	C_f	Nu	C_f	Nu	C_f	Nu
0.0	1.1596	0.2846	0.8958	0.4861	0.6109	0.7205
0.5	1.0685	0.2842	0.8380	0.4860	0.5833	0.7204
1.0	0.9897	0.2839	0.7873	0.4657	0.5583	0.6995
5.0	0.5871	0.2815	0.5150	0.4412	0.4107	0.6733
10.0	0.3167	0.2804	0.3108	0.4211	0.2959	0.6523
15.0	0.1436	0.2790	0.1333	0.3994	0.1267	0.6262
20.0	0.0026	0.2780	-0.0084	0.3777	-0.0021	0.6051
25.0	-0.0813	0.2771	-0.0800	0.3550	-0.1077	0.5790

Table 2 Values of C_f and Nu for different n and ξ (W_e = 0.3, γ = 0.2, Pr = 0.71)

N	ξ = 1.0		ξ = 2.0		ξ = 3.0	
	C_f	Nu	C_f	Nu	C_f	Nu
0.0	1.2047	0.2803	0.8979	0.4856	0.6105	0.7204
0.1	1.1783	0.2816	0.8898	0.4857	0.6071	0.7204
0.2	1.1454	0.2829	0.8780	0.4859	0.6006	0.7205
0.3	1.1032	0.2844	0.8602	0.4860	0.5940	0.7205
0.4	1.0460	0.2859	0.8328	0.4863	0.5812	0.7205
0.5	0.9650	0.2876	0.7881	0.4865	0.5596	0.7206
0.6	0.8433	0.2893	0.7122	0.4868	0.5209	0.7206
0.7	0.6506	0.2912	0.5776	0.4870	0.4477	0.7207
0.8	0.3322	0.2931	0.3311	0.4870	0.2999	0.7208

In vicinity of the lower stagnation point, $\xi \sim 0$ and the boundary layer Eqs. (9) – (10) contract to a system of ordinary differential equations:

$$(1-n)f'''+3ff''-2(f')^2+nW_e f''f'''+\theta=0 \qquad (14)$$

$$\frac{\theta''}{\mathrm{Pr}}+3f\,\theta'=0 \qquad (15)$$

The general model is solved using a powerful and unconditionally stable finite difference technique introduced by Keller (1978). The Keller-box method has a second order accuracy with arbitrary spacing and attractive extrapolation features.

4. NUMERICAL SOLUTION WITH KELLER BOX IMPLICIT METHOD

The governing boundary layer Eqs. (9) – (10) subject to the boundary conditions (11) is solved numerically by using Keller Box implicit differences method. This technique, despite recent developments in other numerical methods, remains a powerful and very accurate approach for parabolic boundary layer flows. It is unconditionally stable and achieves exceptional accuracy (1978). Recently this method has been deployed in resolving many challenging, multi-physical fluid dynamics problems. These include hydromagnetic Sakiadis flow of non-Newtonian fluids (2009), nanofluid transport from a stretching sheet (2011), radiative rheological magnetic heat transfer (2009), water hammer modelling (2005), porous media convection (2008) and magnetized viscoelastic stagnation flows (2009). The Keller-Box discretization is *fully coupled* at each step which reflects the physics of parabolic systems – which are also fully coupled. Discrete calculus associated with the Keller-Box scheme has also been shown to be fundamentally different from all other mimetic (physics capturing) numerical methods, as elaborated by Keller (1978). The Keller Box Scheme comprises four stages.

1. Decomposition of the N^{th} order partial differential equation system to N first order equations.

2. Finite Difference Discretization

3. Quasilinearization of Non-Linear Keller Algebraic Equations and finally.

Table 3 Values of C_f and *Nu* for different γ and ξ (W_e = 0.3, n = 0.2, Pr = 0.71)

γ	ξ = 1.0		ξ = 2.0		ξ = 3.0	
	C_f	*Nu*	C_f	*Nu*	C_f	*Nu*
0.2	1.1032	0.2844	0.8602	0.4860	0.5940	0.7205
0.3	1.5940	0.4979	1.3561	0.8176	0.9738	1.2012
0.4	1.8114	0.6090	1.5815	0.9862	1.1585	1.4412
0.5	1.9350	0.6769	1.7106	1.0882	1.2676	1.5863
0.6	2.0150	0.7226	1.7945	1.1565	1.3396	1.6820
0.7	2.0710	0.7555	1.8533	1.2054	1.3905	1.7503
0.8	2.1124	0.7802	1.8968	1.2422	1.4295	1.8020
0.9	2.1443	0.7996	1.9315	1.2710	1.4592	1.8421
1.0	2.1693	0.8150	1.9580	1.2939	1.4827	1.8741

4. Block-tridiagonal Elimination solution of the Linearized Keller Algebraic Equations.

3. NUMERICAL RESULTS AND DISCUSSION

In order to get a physical insight into the problem, a representative comprehensive set of numerical results are presented in Tables 1 – 4 and Figs. 2 – 9. The numerical problem comprises of two independent variables (ξ, η), two dependent fluid dynamic variables (f, θ) and six thermo-physical and body force control parameters, viz., W_e, n, S_f, S_T, Pr, ξ. The following default parameter values i.e., W_e = n = 0.3, S_f = 0.5, S_T = 1.0, Pr = 0.71, ξ = 1.0 are prescribed (unless otherwise stated). Furthermore, the influence of stream-wise (transverse) coordinate on heat transfer rate is also investigated.

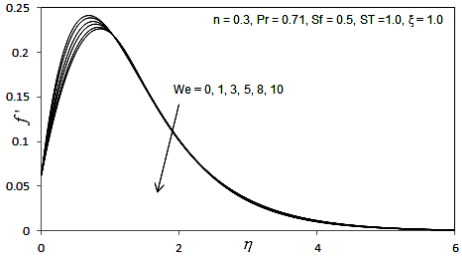

Fig. 2(a). Influence of We on Velocity Profiles.

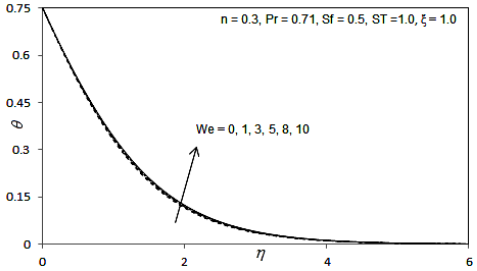

Fig. 2(b). Influence of We on Temperature Profiles.

In Table 1, we present the influence of Weissenberg number (W_e) on skin friction and heat transfer rate (Nusselt number), along with a variation in the traverse coordinate (ξ). Increasing W_e is found to reduce skin friction. For large values of W_e, skin friction is negative. And increasing W_e, also reduces heat transfer rate. Increasing ξ decreases skin friction, whereas increasing ξ , increases heat transfer rate.

Table 2 document results for the influence of *the power law index* (n) on skin friction and heat transfer rate along with a variation in the traverse coordinate (ξ). It is observed that increasing n, decreases skin friction but increases heat transfer rate. Whereas increasing ξ , decreases skin friction but increases heat transfer rate.

Table 3 presents the influence of *the Biot number* (γ) on skin friction and heat transfer rate along with a variation in the traverse coordinate (ξ). It is observed that the increasing γ, increases both the Skin friction and heat transfer rate (Nusselt number). And increasing ξ , decreases the Skin friction but increases the Nusselt number.

Table 4 documents results for the influence of *the Prandtl number* (Pr) on skin friction and heat transfer rate along with a variation in the traverse coordinate (ξ). It is observed that increasing Pr, decelerates skin friction but accelerates heat transfer rate. And increasing ξ , decreases skin friction but increases heat transfer rate.

Figures 2(a) – 2(b) depict the velocity (f') and temperature (θ) distributions with increasing *Weissenberg number, We*. Very little tangible effect is observed in fig. 2a, although there is a very slight decrease in velocity with increase in *We*. Conversely, there is only a very slight increase in temperature magnitudes in Fig. 2(b) with a rise in *We*. The mathematical model reduces to the *Newtonian viscous flow model* as $We \to 0$ and $n \to 0$. The momentum boundary layer equation in this case contracts to the

Table 4: Values of C_f and *Nu* for different Pr and ξ (W_e = 0.3, n = 0.3, γ = 0.2)

Pr	ξ = 1.0		ξ = 2.0		ξ = 3.0	
	C_f	*Nu*	C_f	*Nu*	C_f	*Nu*
0.5	1.2598	0.2184	1.1381	0.3483	0.8359	0.5076
0.7	1.1098	0.281	0.8711	0.4794	0.6024	0.7103
1.0	1.1718	0.5101	0.8242	0.9097	0.5620	1.3522
2.0	0.7641	0.9396	0.4174	1.8147	0.2817	2.7003
3.0	0.5353	1.33922	0.2775	2.7195	0.1865	4.0472
5.0	0.3212	2.3163	0.1637	4.5291	0.1090	6.7423
7.0	0.2268	3.2426	0.1139	6.3409	0.0748	9.4408
8.0	0.1969	3.7064	0.0981	7.2470	0.0638	10.7911
10.0	0.1543	4.6360	0.0752	9.0596	0.0478	13.4891

familiar equation for *Newtonian mixed convection* from a plate, viz.

$$f'''+(3f+\xi)f''-2f'^{2}+\theta=\xi\left(f'\frac{\partial f'}{\partial \xi}-f''\frac{\partial f}{\partial \xi}\right)$$

The thermal boundary layer equation (10) remains unchanged.

Figures 3(a) - 3(b) illustrates the effect of the *power law index*, *n*, on the velocity (f') and temperature (θ) distributions through the boundary layer regime. Velocity is increased with increasing *n*. Conversely temperature is consistently reduced with increasing values of *n*.

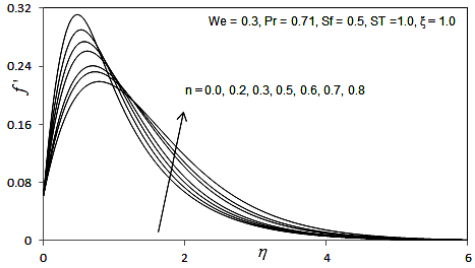

Fig. 3(a). Influence of n on Velocity Profiles.

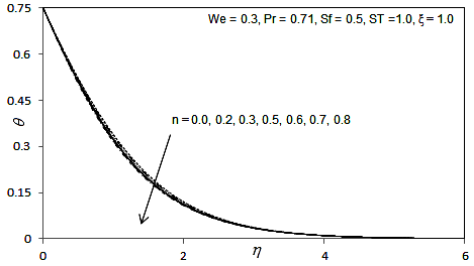

Fig. 3(b). Influence of n on Temperature Profiles.

Figures 4(a) - 4(b) depict the evolution of velocity (f') and temperature (θ) functions with a variation in velocity slip parameter, S_f. Dimensionless velocity component (Fig. 4a) is considerably enhanced with increasing S_f. In Fig. 4b, an increase in S_f is seen to considerably reduce temperatures throughout the boundary layer regime. The influence of S_f is evidently more pronounced closer to the sphere surface (η = 0). Further from the surface, there is a transition in *velocity slip effect*, and the flow is found to be accelerated markedly. Smooth increase in the velocity profiles are observed into the free stream demonstrating excellent convergence of the numerical solution. Furthermore, the acceleration near the wall with increasing velocity slip effect has been computed by Crane and McVeigh (2002) using asymptotic methods, as has the retardation in flow further from the wall. The switch in velocity slip effect on velocity evolution has also been observed for the case of a power-law rheological fluid by O. Ajadi *et al.* (2009). Fig. 4(b) shows that an increase in S_f, significantly reduces temperature. Temperature profiles consistently decay monotonically from a maximum at the sphere surface to the free stream. All profiles converge at large value of radial coordinate, again showing that convergence has been achieved in the numerical computations.

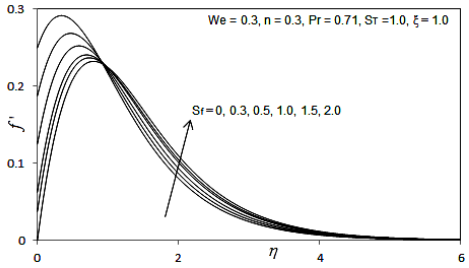

Fig. 4(a). Influence of S_f on Velocity Profiles.

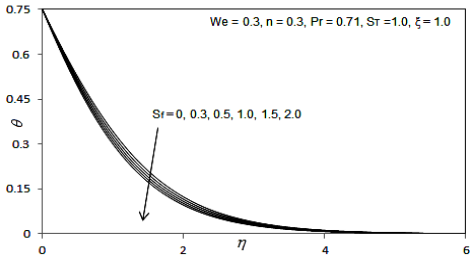

Fig. 4(b). Influence of Sf on Temperature Profiles.

Figures 5(a) - 5(b) depict the evolution of velocity (f') and temperature (θ) functions with a variation in thermal jump parameter, S_T. The response of velocity is much more consistent than for the case of changing velocity slip parameter (Fig. 5(a)). It is strongly decreased for all locations in the radial direction. The peak velocity accompanies the case of no thermal jump (S_T = 0). The maximum deceleration corresponds to the case of strongest thermal jump (S_T = 3). Temperatures (Fig. 5(b)) are also strongly depressed with increasing thermal jump. The maximum effect is observed at the wall. Further into the free stream, all temperature profiles converge smoothly to the vanishing value. The numerical computations correlate well with the results of Larrode *et al.* (2000) who also found that temperature is strongly lowered with increasing thermal jump and that this is attributable to the decrease in heat transfer from the wall to the fluid regime, although they considered only a Newtonian fluid.

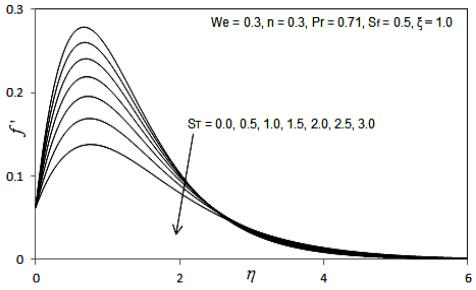

Fig. 5(a). Influence of S_T on Velocity Profiles.

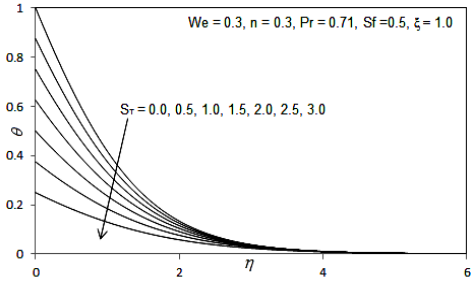

Fig. 5(b). Influence of St on Temperature Profiles.

Figures 6(a) – 6(b) depicts the velocity (f') and temperature (θ) distributions with radial coordinate, for various transverse (stream wise) coordinate values, ξ along with the variation in the Weissenberg number (W_e). Clearly, from these figures it can be seen that as suction parameter ξ increases, the maximum fluid velocity decreases. This is due to the fact that the effect of the suction is to take away the warm fluid on the vertical plate and thereby decrease the maximum velocity with a decrease in the intensity of the natural convection rate. Fig. 6(b) shows the effect of the local suction parameter on the temperature profiles. It is noticed that the temperature profiles decrease with an increase in the suction parameter and as the suction is increased, more warm fluid is taken away and this the thermal boundary layer thickness decreases. It is also seen that an increase in W_e, the impedance offered by the fibers of the porous medium will increase and this will effectively decelerate the flow in the regime, as testified to by the evident decrease in velocities shown in Fig. 6(a).

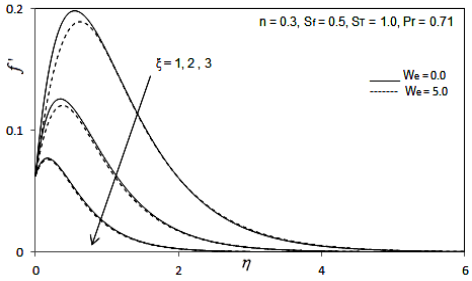

Fig. 6(a). Influence of ξ and W_e on Velocity Profiles.

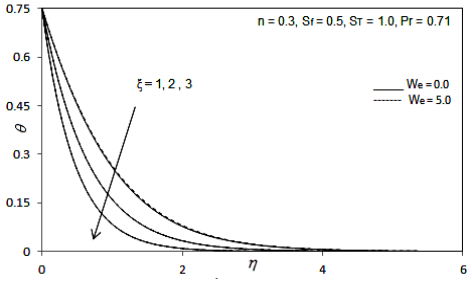

Fig. 6(b). Influence of ξ and W_e on Temperature Profiles.

Figures 7(a) – 7(b) depict the velocity (f') and temperature (θ) distributions with radial coordinate, for various transverse (stream wise) coordinate values, ξ along with the variation in the power law index (n). Clearly, from these figures it can be seen that as suction parameter ξ increases, the maximum fluid velocity decreases. This is due to the fact that the effect of the suction is to take away the warm fluid on the vertical plate and thereby decrease the maximum velocity with a decrease in the intensity of the natural convection rate. Fig. 7(b) shows the effect of the local suction parameter on the temperature profiles. It is noticed that the temperature profiles decrease with an increase in the suction parameter and as the suction is increased, more warm fluid is taken away and this the thermal boundary layer thickness decreases. It is also seen that an increase in *n*, the impedance offered by the fibers of the porous medium will increase and this will effectively decelerate the flow in the regime, as testified to by the evident decrease in velocities shown in Fig. 7(a).

Figures 8(a) – 8(b) depict the velocity (f') and temperature (θ) distributions with radial coordinate, for various transverse (stream wise) coordinate values, ξ along with the variation in the velocity slip (S_f). Clearly, from these figures it can be seen that as suction parameter ξ increases, the

maximum fluid velocity decreases. This is due to the fact that the effect of the suction is to take away the warm fluid on the vertical plate and thereby decrease the maximum velocity with a decrease in the intensity of the natural convection rate. Fig. 8(b) shows the effect of the local suction parameter on the temperature profiles. It is noticed that the temperature profiles decrease with an increase in the suction parameter and as the suction is increased, more warm fluid is taken away and this the thermal boundary layer thickness decreases. It is also seen that an increase in S_f, the impedance offered by the fibers of the porous medium will increase and this will effectively decelerate the flow in the regime, as testified to by the evident decrease in velocities shown in Fig. 8(a).

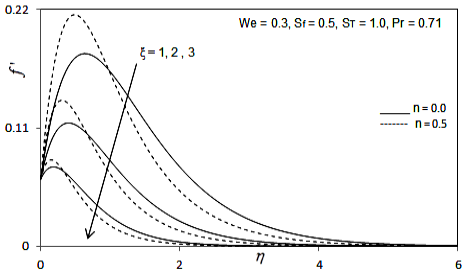

Fig. 7(a). Influence of ξ and n on Velocity Profiles.

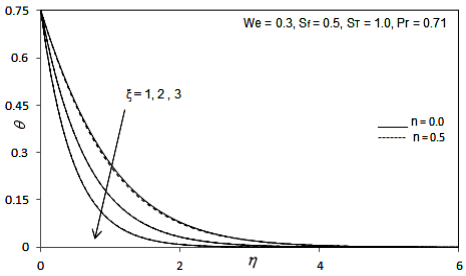

Fig. 7(b). Influence of ξ and n on Temperature Profiles.

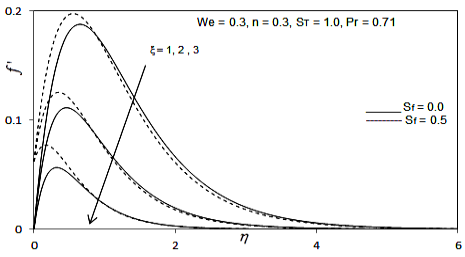

Fig. 8(a). Influence of ξ and S_f on Velocity Profiles.

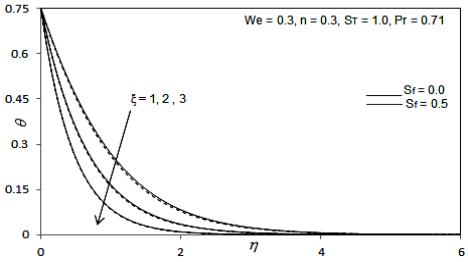

Fig. 8(b). Influence of ξ and S_f on Temperature Profiles.

Figures 9(a) – 9(b) depict the velocity (f') and temperature (θ) distributions with radial coordinate, for various transverse (stream wise) coordinate values, ξ along with the variation in the Thermal jump (S_T). Clearly, from these figures it can be seen that as suction parameter ξ increases, the maximum fluid velocity decreases. This is due to the fact that the effect of the suction is to take away the warm fluid on the vertical plate and thereby decrease the maximum velocity with a decrease in the intensity of the natural convection rate. Fig. 9(b) shows the effect of the local suction parameter on the temperature profiles. It is noticed that the temperature profiles decrease with an increase in the suction parameter and as the suction is increased, more warm fluid is taken away and this the thermal boundary layer thickness decreases. It is also seen that an increase in S_T, the impedance offered by the fibers of the porous medium will increase and this will effectively decelerate the flow in the regime, as testified to by the evident decrease in velocities shown in Fig. 9(a).

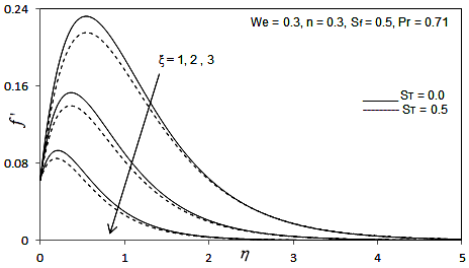

Fig. 9(a). Influence of ξ and S_T on Velocity Profiles.

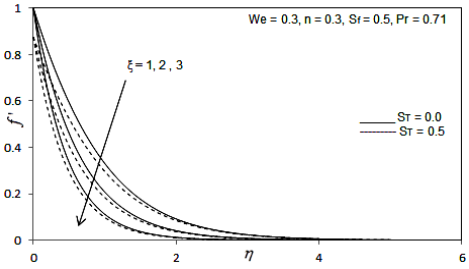

Fig. 9(b). Influence of ξ and S_T on Temperature Profiles.

4. CONCLUSIONS

Numerical solutions have been presented for the buoyancy-driven flow and heat transfer of Tangent Hyperbolic flow external to a vertical porous plate. The Keller-box implicit second order accurate finite difference numerical scheme has been utilized to efficiently solve the transformed, dimensionless velocity and thermal boundary layer equations, subject to realistic boundary conditions. Excellent correlation with previous studies has been demonstrated testifying to the validity of the present code. The computations have shown that:

1. Increasing Weissenberg number, W_e, reduces velocity, skin friction (surface shear stress)

and heat transfer rate, whereas it elevates temperature in the boundary layer.

2. Increasing power law index, *n*, increases velocity and Nusselt number for all values of radial coordinate i.e., throughout the boundary layer regime whereas it depresses temperature and skin friction.

3. Increasing velocity slip, S_f, increases velocity and heat transfer rate but decreases temperature and skin friction (surface shear stress).

4. Increasing thermal jump, S_T, decreases velocity, temperature, skin friction and hear transfer rate.

5. Increasing transverse coordinate (ζ) along with increase in the Weissenberg number (W_e), generally decelerates the flow near the plate surface and reduces momentum boundary layer thickness and also reduces temperature and therefore decreases thermal boundary layer thickness in Tangent Hyperbolic non-Newtonian fluids.

6. Increasing transverse coordinate (ζ) along with increase in the power law index (n), generally decelerates the flow near the plate surface and reduces momentum boundary layer thickness and also reduces temperature and therefore decreases thermal boundary layer thickness in Tangent Hyperbolic non-Newtonian fluids.

REFERENCES

Abbas, Z., Y. Wang, T. Hayat and M. Oberlack (2009). Slip effects and heat transfer analysis in a viscous fluid over an oscillatory stretching surface. *International Journal for Numerical Methods in Fluids* 59(4), 443–458.

Abdul gaffar S, V. Ramachandra Prasad and O. Anwar Beg (2015). Computational Analysis of Magnetohydrodynamic Free Convection Flow and Heat Transfer of Non-Newtonian Tangent Hyperbolic Fluid from a Horizontal Circular cylinder with Partial Slip. *Int. J. of Applied and Computational Mathematics.*

Abdul gaffer, S, V. Ramachandra Prasad, E. Keshava Reddy and O. Anwar Beg (2014). Free Convection Flow and Heat Transfer of Non-Newtonian Tangent Hyperbolic Fluid from an Isothermal Sphere with Partial Slip. *Arabian Journal for Science and Engineering 39(11), 8157-8174.*

Abdul gaffer, S, V. Ramachandra Prasad and O. Anwar Beg (2015). Numerical study of flow and heat transfer of non-Newtonian Tangent Hyperbolic fluid from a sphere with Biot number effects. *Alexandria Engineering Journal.*

Ajadi, S. O., Adegoke A. and A. Aziz (2009). Slip boundary layer flow of non-Newtonian fluid over a flat plate with convective thermal boundary condition. *Int. J. Nonlinear Science 8(3), 300-306.*

Akbar, N. S., S. Nadeem, R. U. Haq and Z. H. Khan (2013). Numerical solution of Magnetohydrodynamic boundary layer flow of tangent hyperbolic fluid towards a stretching sheet. *Indian J. Phys* 87(11), 1121-1124.

Akram, S. and N. Sohail (2012). Simulation of heat and mass transfer on peristaltic flow of hyperbolic tangent fluid in an asymmetric channel. *Int. J. Numer. Meth. Fluids 70(12), 1475-1493.*

Andersson, H. I. (2002). Slip flow past a stretching surface. *Acta Mechanica* 158(1-2), 121–125.

Anwar Bég, O., J. Zueco and L. M. Lopez-Ochoa (2011). Network numerical analysis of optically thick hydromagnetic slip flow from a porous spinning disk with radiation flux, variable thermophysical properties, and surface injection effects. *Chemical Engineering Communications* 198(3), 360-384.

Anwar Bég, O., K. Abdel Malleque and M. N. Islam (2012). Modelling of Ostwald-deWaele non-Newtonian flow over a rotating disk in a non-Darcian porous medium. *Int. J. Applied Mathematics and Mechanics* 8, 46-67.

Anwar Hossain, M., K. Khanafer and K. Vafai (2001). The effect of radiation on free convection flow with variable viscosity from a porous vertical plate. Int. J. Therm. Sci. 40, 115-124.

Ariel, P. D. (2008). Two dimensional stagnation pointflow of an elastic - viscous fluid with partial slip. *Zeitschrift für angewandte Mathematik und Mechanik* 88, 320–324.

Ariel, P. D., T. Hayat and S. Asghar (2006). The flow of an elasticoviscous fluid past a stretching sheet with partial slip. *Acta Mechanica* 187, 29–35.

Chauhan, D. S. and A. Olkha (2011). Slip flow and heat transfer of a second-grade fluid in a porous medium over a stretching sheet with power-law surface temperature or heat flux. *Chemical Engineering Communication* 198, 1129–1145.

Chen, C. H. (2009). Magneto-hydrodynamic mixed convection of a power-law fluid past a stretching surface in the presence of thermal radiation and internal heat generation/absorption. *Int. J. Non-Linear Mechanics* 44, 596-603.

Clarke, J. F. (1973). Transpiration and natural convection: the vertical flat plate problem. *Journal of fluid Mechanics 57, 45-61.*

Clarke, J. F. and N. Riley (1975). Natural convection induced in a gas by the presence of a hot porous horizontal surface. *Q. J. Mech. Appl. Math. 28, 373-396.*

Clarke, J. F. and N. Riley (1976). Free convection and the burning of a horizontal fuel surface. *Journal of Fluid Mechanics 74, 415-431.*

Crane, L. J. and A. G. McVeigh (2010). Slip flow on a microcylinder. *Z. Angew. Math. Phys* 61(3), 579-582.

Crane, L. J. and A. G. McVeigh (2010). Uniform slip flow on a cylinder. *PAMM: Proc. Appl. Math. Mech.* 10(1), 477-478.

Gad-el-Hak, M. (1999). The Fluid Mechanics of Micro devices: The Freeman Scholar Lecture. *Journal of Fluids Engineering* 121(1), 5–33.

Gombosi, T. A. (2002). *Gaskinetic Theory,* Cambridge Univ. Press, Cambridge, England, U.K.

Ho, C. M. and Y. C. Tai (1998). Micro-Electro-Mechanical-Systems (MEMS) and Fluid Flows. *Annual Review of Fluid Mechanics* 30, 579–612.

Inman, R. M. (1964). Heat transfer for laminar slip flow of a rarefied gas in a parallel plate channel or a circular tube with uniform wall temperature. *NASA Tech. Report, D-2213*.

Keller H. B. (1978). Numerical methods in boundary-layer theory. *Ann. Rev. Fluid Mech*. 10, 417-433.

Kumari, M., G. Nath (2009). Steady mixed convection stagnation-point flow of upper convected Maxwell fluids with magnetic field. *Int. J. Nonlinear Mechanics* 44, 1048-1055.

Larrode, F. E, C. Housiadas and Y. Drossinos (2000). Slip-flow heat transfer in circular tubes. *Int. J. Heat Mass Transfer* 43(15), 2669-2680.

Lin, H. T. and Yu. W. S. (1988). Free convection on a horizontal plate with blowing and suction. *Transaction of ASME Journal of Heat Transfer 110(3), 793-796.*

Lin, T. C. and S. A. Schaaf (1951). Effect of Slip on Flow Near a Stagnation Point and in a Boundary Layer. *NACATN*-2568.

Malvandi, A., F. Hedayati and D. Ganji (2015). Boundary layer slip flow and heat transfer of Nanofluid induced by a permeable stretching sheet with convective boundary condition. *Journal of Applied Fluid Mechanics* 8(1), 151-158.

Maslen, S. H. (1952). Second Approximation to Laminar Compressible Boundary Layer on Flat Plate in Slip Flow. *NACATN*-2818.

Maslen, S. H. (1963). Second-Order Effects in Laminar Boundary Layers. *AIAA Journal* 1(1), 33–40.

Merkin J. H. (1972). Free convection with blowing and suction. *International Journal of Heat Mass Transfer 15(5), 989-999.*

Merkin, H. J. (1975). The effects of blowing and suction on free convection boundary layers. *International Journal of Heat Mass Transfer 18(2), 237-244.*

Mukhopadhyay, S., Md. S. Uddin and G. C. Layek (2012). Lie group analysis of MHD boundary layer slip flow past a heated stretching sheet in presence of heat source/sink. *International Journal of Applied Mathematics and Mechanics* 8(16), 51-66.

Nadeem, S. and S. Akram (2009). Peristaltic transport of a hyperbolic tangent fluid model in an asymmetric channel. *ZNA 64a, 559–567.*

Nadeem, S. and S. Akram (2011). Magnetohydrodynamic peristaltic flow of a hyperbolic tangent fluid in a vertical asymmetric channel with heat transfer. *Acta Mech. Sin. 27(2), 237–250.*

Norouzi, M., M. Davoodi, O. Bég, Anwar and A. A. Joneidi (2013). Analysis of the effect of normal stress differences on heat transfer in creeping viscoelastic Dean flow. *Intl. J. Thermal Sciences* 69, 61-69.

Orhan, A. and A. Kaya (2008). Non-Darcian forced convection flow of viscous dissipating fluid over a flat plate embedded in a porous medium. *Transport in Porous Media* 73(2), 173-186.

POP, I. and D. B. INGHAM (2001). *Convective Heat Transfer: Mathematical and Computational Modelling of Viscous Fluids and Porous Media*. Pergamon, Amsterdam, NewYork.

Prasad, V. R, B. Vasu, O. Anwar Bég and D. R. Parshad (2012). Thermal radiation effects on magnetohydrodynamic free convection heat and mass transfer from a sphere in a variable porosity regime. *Comm. Nonlinear Science Numerical Simulation* 17(2), 654–671.

Prasad, V. R., B. Vasu, O. Anwar Bég and R. Parshad (2011). Unsteady free convection heat and mass transfer in a Walters-B viscoelastic flow past a semi-infinite vertical plate: a numerical study. *Thermal Science-International Scientific J.* 15(2), 291-305.

Rashidi, M. M, O. Anwar Bég and M. T. Rastegari (2012). A study of non-Newtonian flow and heat transfer over a non-isothermal wedge using the Homotopy Analysis Method. *Chemical Engineering Communications* 199(2), 231-256.

Saghafian, M., I. Saberian, R. Rajabi and E. Shirani (2015). A numerical study on slip flow heat transfer in micro-poiseuille flow using perturbation method. *Journal of Applied Fluid Mechanics* 8(1), 123-132.

Sparrow, E. M. and S. H. Lin (1962). Laminar heat transfer in tubes under slip-flow conditions. *ASME J. Heat Transfer* 84(4), 363-639.

Sparrow, E. S. and R. D. Cess (1961). Free convection with blowing or suction. Journal of Heat Transfer 83(4), 387-396.

Spillane, S. (2007*). A study of boundary layer flow with no-slip and slip boundary conditions*.

PhD Thesis, Dublin Inst. of Technology, Ireland.

Steffe J. F. (2001). *Rheological methods in Food Process Engineering*, 2nd edn, Freeman Press, Michigan, USA.

Subhas Abel, M., P. S. Datti and N. Mahesha (2009). Flow and heat transfer in a power-law fluid over a stretching sheet with variable thermal conductivity and non-uniform heat source. *Int. J. Heat Mass Transfer* 52(11-12), 2902-2913.

Swati, M. and H. I. Anderson (2009). Effects of slip and heat transfer analysis of flow over an unsteady stretching surface. *Heat and Mass Transfer 45(11), 1447-1452.*

Swati, M. and R. S. Reddy Gorla (2011). Effects of partial slip on boundary layer flow past a permeable exponential stretching sheet in presence of thermal radiation. *Heat Mass Transfer 45(11), 1447–1452.*

Tripathi, D., O. Anwar Bég and J. Curiel-Sosa (2012). Homotopy semi-numerical simulation of peristaltic flow of generalized Oldroyd-B fluids with slip effects. *Computer Methods in Biomechanics Biomedical Engineering.* 17(4), 433-442.

Vajravelu, K., K.V. Prasad, J. Lee, C. Lee, I. Pop and Rob (2011). A. Van Gorder, Convective heat transfer in the flow of viscous Ag–water and Cu–water nanofluids over a stretching surface*. Int. J. Thermal Sciences* 50(5), 843-851.

Van Dyke, M. (1969). Higher Order Boundary Layer Theory. *Annual Review of Fluid Mechanics* 1, 265–292.

Vedhanayagam, M., Altenkirch, R. A. and R. Eichhorn (1980). A transformation of the boundary layer equations for the free convection past a vertical flat plate with arbitrary blowing and suction wall temperature variations. *International Journal of Heat Mass Transfer 23, 1286-1288.*

Wang, C. Y. (2002). Flow due to a stretching boundary with partial slip — an exact solution of the Navier-Stokes equations. *Chemical Engineering Sciences* 57(17), 3745–3747.

Wang, C. Y. and Ng C. O. (2011). Slip flow due to a stretching cylinder. *Int. J. Non-Linear Mechanics* 46(9), 1191-1194.

Wilson, L. L, A. Speers and M. A. Tung (1993). Yield stresses in molten chocolates. *J. Texture Studies* 24(3), 269–286.

Wuest, W. (1967). Boundary Layers in Rarefied Gas Flow. *Progress in Aerospace Sciences* 8, 295–352.

Yoshimura, A. and R. K. Prudhomme (1998). Wall slip corrections for couette and parallel disc viscometers. *Journal of Rheology.* 32, 53–67.

Yu, S. P. and T. A. Ameel (2002). Slip-flow convection in isoflux rectangular microchannel. *ASME J. Heat Transfer* 124(2), 346-355.

Zhang, Y. L. and K. Vairavamoorthy (2005). Analysis of transient flow in pipelines with fluid–structure interaction using method of lines. *Int. J. Num. Meth. Eng* 63(10), 1446-1460.